

# Green Chemistry

Accepted Manuscript



This is an *Accepted Manuscript*, which has been through the Royal Society of Chemistry peer review process and has been accepted for publication.

*Accepted Manuscripts* are published online shortly after acceptance, before technical editing, formatting and proof reading. Using this free service, authors can make their results available to the community, in citable form, before we publish the edited article. We will replace this *Accepted Manuscript* with the edited and formatted *Advance Article* as soon as it is available.

You can find more information about *Accepted Manuscripts* in the [Information for Authors](#).

Please note that technical editing may introduce minor changes to the text and/or graphics, which may alter content. The journal's standard [Terms & Conditions](#) and the [Ethical guidelines](#) still apply. In no event shall the Royal Society of Chemistry be held responsible for any errors or omissions in this *Accepted Manuscript* or any consequences arising from the use of any information it contains.



[www.rsc.org/greenchem](http://www.rsc.org/greenchem)



Journal Name

ARTICLE

## New insights into the curing of epoxidized linseed oil with dicarboxylic acids†

Cheng Ding,<sup>a</sup> Peter S. Shuttleworth,<sup>b</sup> Sarah Makin,<sup>a</sup> James H. Clark<sup>a</sup> and Avtar S. Matharu<sup>\*a</sup>

Received 00th January 20xx,  
Accepted 00th January 20xx

DOI: 10.1039/x0xx00000x

www.rsc.org/

The effect of systematically increasing chain length of a series of linear  $\alpha$ ,  $\omega$ -dicarboxylic acids (DCAs) from C<sub>6</sub> to C<sub>18</sub> diacids and a cyclic diacid, Pripol 1009F, on thermal and mechanical properties of the resultant epoxy thermosets derived from epoxidized linseed oil (ELO) are reported. Different techniques including differential scanning calorimetry (DSC), solvent extraction, FT-IR, NMR, dynamic mechanical analysis (DMA), tensile tests and thermogravimetric analysis (TGA) are used in this study. The results indicated that the obtained epoxy resins were highly crosslinked polymers with only a small fraction of low molecular weight soluble materials. The glass transition temperature ( $T_g$ ), tensile strength, Young's modulus, elongation at break and toughness decreased while the thermal stability increased with respect to increasing chain length of DCAs. Interestingly, strain hardening was only observed for adipic acid (C<sub>6</sub>) sample for which the best mechanical properties observed.

### Introduction

In an era of declining petroleum resources and increasing environmental concerns associated with continued manufacturing of petroleum-derived products, new developments in biobased products are gaining significant or renewed interest in order to help mitigate such concerns.<sup>1-3</sup> Biobased- or bioderived-polymers, i.e., those derived from (bio)renewable feedstocks, represent a significant opportunity for development as there are less than 1% of such polymers available on the market globally.<sup>4</sup> Importantly, as policy and legislative initiatives come to the fore, such as Lead Market Initiative (European Union)<sup>5</sup> and BioPreferred (USA),<sup>6</sup> the demand for bio-based polymers will increase tremendously. Compared to the rapid development of thermoplastic polymers from renewable resources which have a market share of over 80%, research on bio-based thermosetting materials has received much less recent attention.<sup>7</sup>

Epoxy resins are an important class thermosets due to their excellent dimensional and thermal stability, and ease of processability.<sup>8</sup> Auvergne *et al.*<sup>9</sup> recently reviewed various renewable materials that were exploited to develop bio-based epoxy prepolymer and hardeners (curing agents) including polyphenols, lignin, starch, sugar, vegetable oils, terpenes and resin acids. Among these, vegetable oils are of great importance in producing bio-based epoxy resins due to their

availability and inherent unsaturation which can be chemically exploited. For example, linseed- and soybean-oil may be epoxidized across their double bonds; epoxidized linseed oil (ELO) has higher oxirane content than epoxidized soybean oil (ESBO) due to a higher degree of unsaturation.

Carboxylic acids or polyesters and anhydrides are the second most important class of epoxy curing agents after amines. Short-chain dicarboxylic acids (DCAs) may be obtained either by fermentation or chemical transformation of carbohydrates whilst long-chain DCAs could be obtained either by chemical or enzymatic modification of fatty acids. In 2004, the US Department of Energy (DOE) proposed 15 target chemicals derived from biomass (platform molecules) worthy of industrial exploitation, eight of which are DCAs accessible by fermentation of sugars, mostly glucose.<sup>10-16</sup> With an increased availability of bio-derived carboxylic acids, for example, adipic acid, sebacic acid and dodecanoic acid produced by Verdezyne, coupled with ready availability of vegetable plant oils merits a re-investigation of a full systematic study of the properties of the resultant biobased epoxy thermosets. Shimbo *et al.*<sup>17</sup> have reported the effect of different DCAs on the fatigue behavior of epoxy resins but the latter were derived from petroleum-based epoxy prepolymer diglycidyl ether of bisphenol A (DGEBA). There are relatively few comprehensive literature reports with respect to bioderived or platform molecule DCAs (citric acid, succinic acid, adipic acid and sebacic acid) as curing agents with epoxy systems acids. For example, Shogren *et al.*<sup>18</sup> reported sebacic acid to crosslink DGEBA or diglycidyl ether of 4, 4'-dihydroxybiphenol (DGE-DHBP) to develop liquid-crystal elastomers with exchangeable links. Plant oil-derived dimer acid Pripol 1009 and trimer acid Pripol 1040 have also been studied with ELO to make flexible thermoset resins<sup>19</sup> or with DGEBA to make "vitrimers", i.e. strong organic glass covalent

<sup>a</sup> Green Chemistry Centre of Excellence, Department of Chemistry, University of York, York YO10 5DD, England, UK. E-mail: avtar.matharu@york.ac.uk

<sup>b</sup> Departamento de Física de Polímeros, Elastómeros y Aplicaciones Energéticas, Instituto de Ciencia y Tecnología de Polímeros, CSIC, c/ Juan de la Cierva 3, 28006, MADRID.

† Electronic Supplementary Information (ESI) available. See DOI: 10.1039/x0xx00000x

formers that able to change their topology through thermoactivated bond exchange reactions.<sup>20-22</sup>

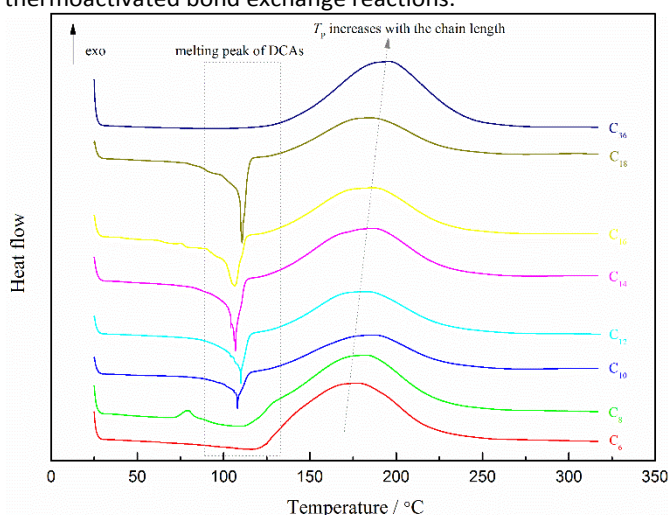


Fig. 1 DSC thermograms of ELO with different DCAs at a heating rate of  $10\text{ }^{\circ}\text{C min}^{-1}$ .

Herein, we report a timely comprehensive study of the effect on systematically extending the chain length of a series of  $\alpha$ ,  $\omega$ -

DCAs (even carbon number DCAs from  $C_6$  to  $C_{18}$  and a bio-derived  $C_{36}$  diacid Pripol 1009F) on the physical and mechanical properties of the resultant biobased ELO crosslinked systems in order to enhance knowledge that leads to a future need for more biobased products.

## Results and discussion

In this study, ELO-based thermoset resins were prepared by crosslinking ELO with different DCAs in the presence of DMAP as accelerator.

### DSC analysis

Dynamic DSC analysis was used to study the cure process and to determine the activation energy ( $E_a$ ).

Fig. 1 shows the DSC thermograms of the epoxy mixtures (obtained after premixing) at heating rate of  $10\text{ }^{\circ}\text{C min}^{-1}$ . The first endotherm at around 100 to 125  $^{\circ}\text{C}$  is attributed to the melting of the DCAs before the exothermic transition which is associated with the curing process. This curing process in most cases starts immediately after the DCAs have melted. For the  $C_6$  sample, the melting transition of adipic acid was not as

obvious as the others probably due to its higher initial reactivity during the premixing stage.

The total enthalpy of curing  $\Delta H_T$  and peak temperature of the exothermic curing peak  $T_p$  at different heating rates are listed in Table 1 and Table S1. It can be seen that  $T_p$  increases with heating rate and DCA chain length. The higher  $T_p$  with increased heating rate is attributed to the thermal lag caused by higher heating rate as reported by Haines.<sup>23</sup> The total enthalpy released during the curing reaction decreased with the increase of chain length. Chiu *et al.*<sup>24</sup> also showed a similar trend for the curing process of sulfone epoxy monomers with different amine curing agents, i.e., amine curing agents with longer chain lengths generated lower  $\Delta H_T$  whilst  $T_p$  shifted to higher values. The increased  $T_p$  and decreased  $\Delta H_T$  is probably due to a higher probability of entanglement of the polymeric or oligomeric chains with increasing chain length which would increase the steric hindrance of the curing reaction and thus decrease curing reactivity.

The activation energy ( $E_a$ ) of the curing process was determined using the Kissinger method (eq. (1))

$$\frac{d(\ln(q/T_p^2))}{d(1/T_p)} = -\frac{E_a}{R} \quad (1)$$

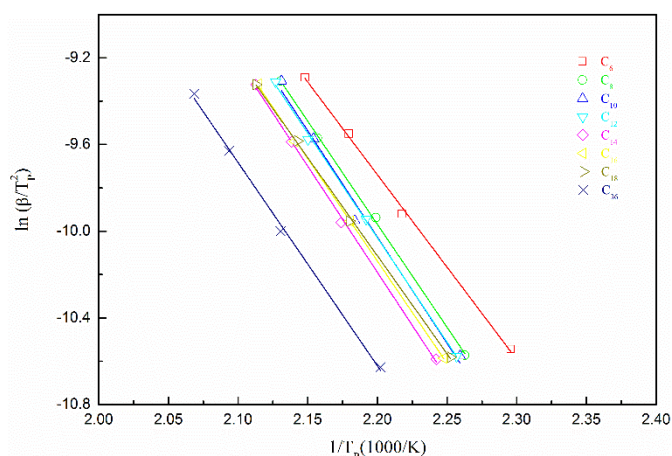
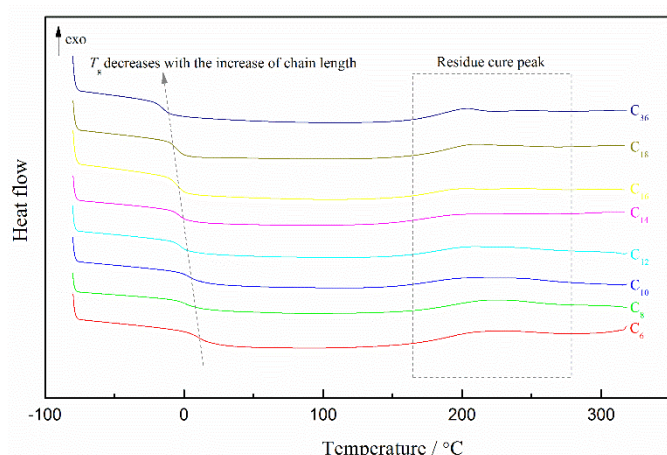
where  $R$  is the universal gas constant, by plotting of  $\ln(q/T_p^2)$  versus  $1/T_p$  as shown in Fig. 2 (Kissinger plot), whereby the gradient corresponds to  $E_a$ . The Kissinger plots show good linearity for all DCAs studied with  $E_a$  in the range 70 to 85  $\text{kJ mol}^{-1}$ . Adipic acid ( $C_6$ ) gave the lowest  $E_a$  which further suggests its fast reactivity with ELO in the presence of DMAP as an accelerator. Ghodsieh *et al.*<sup>25</sup> reported the curing kinetics of epoxy resin mixtures based on DGEBA and ESBO with  $C_{10}$  sebacic acid. The activation energies recalculated based on the Kissinger method ranged from 50-64  $\text{kJ mol}^{-1}$  which were lower compared with our results probably due to the fact that the glycidyl groups in DGEBA are disposed terminally rather than internally as is the case for our epoxidized vegetable oils, thus are more reactive due to the less steric hindrance.

Fig. 3 shows the  $T_g$  of films obtained by curing ELO with different DCAs at 160  $^{\circ}\text{C}$  for 1 h. With increasing DCA chain length,  $T_g$  decreased from 7.0  $^{\circ}\text{C}$  for  $C_6$  to -15.1  $^{\circ}\text{C}$  of  $C_{36}$  probably due to the decrease in crosslink density. Shorter crosslinkers lack flexibility and form tighter or closer crosslinked networks.

**Table 1.** Thermal properties of ELO-DCAs systems and data related to the extracted soluble substances from their polymers.

| Sample          | $\Delta H_T$ [J g <sup>-1</sup> ] | $E_a$ [kJ mol <sup>-1</sup> ] | $T_g$ [°C] | $\Delta H_R$ [J g <sup>-1</sup> ] | Degree of cure (%) <sup>a</sup> | Soluble [wt%] | $M_w$ |
|-----------------|-----------------------------------|-------------------------------|------------|-----------------------------------|---------------------------------|---------------|-------|
| C <sub>6</sub>  | 254.9±4.9                         | 70.7±0.7                      | 7.0        | 23.7                              | 90.7                            | 1.85±0.05     | 2935  |
| C <sub>8</sub>  | 235.6±6.2                         | 78.9±1.8                      | 3.7        | 30.4                              | 87.1                            | 1.96±0.05     | 2271  |
| C <sub>10</sub> | 251.6±4.8                         | 82.9±3.9                      | 0.4        | 25.5                              | 89.9                            | 1.87±0.04     | 2288  |
| C <sub>12</sub> | 260.9±14.4                        | 79.2±1.0                      | -2.2       | 22.2                              | 91.5                            | 1.78±0.06     | 2396  |
| C <sub>14</sub> | 235.9±16.1                        | 81.3±0.5                      | -3.6       | 11.3                              | 95.2                            | 1.74±0.01     | 2460  |
| C <sub>16</sub> | 232.4±7.0                         | 78.6±7.7                      | -5.0       | 11.2                              | 95.8                            | 1.53±0.06     | 2436  |
| C <sub>18</sub> | 235.3±12.2                        | 75.3±4.3                      | -5.5       | 13.7                              | 94.2                            | 1.74±0.04     | 2638  |
| C <sub>36</sub> | 172.9±2.6                         | 78.9±4.4                      | -15.1      | 13.2                              | 92.3                            | 3.05±0.01     | 2487  |

<sup>a</sup> Degree of cure or conversion =  $(\Delta H_T - \Delta H_R) / \Delta H_T$

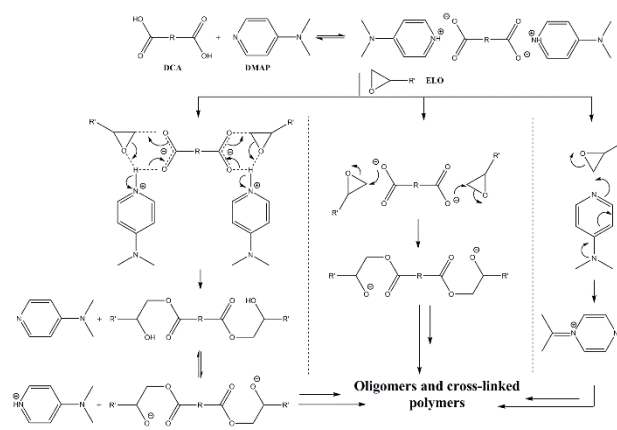
**Fig. 2** Kissinger plot to determine activation energy ( $E_a$ ).**Fig. 3** DSC thermograms of cured ELO-DCAs films at 160 °C for 1 h.

With the increase of crosslink density, the free volume within the resin system decreased thus the motion of the

network segments in samples with high crosslink density was restricted, which was responsible for the increase of  $T_g$ .

A similar trend was observed by Shimbo *et al.*<sup>17,26</sup> who studied properties of epoxy networks of DGEBA cured with different DCAs (C<sub>4</sub>, C<sub>6</sub>, C<sub>10</sub>, C<sub>12</sub>)<sup>17</sup> and different aliphatic  $\alpha,\omega$ -diamines (C<sub>2</sub>, C<sub>4</sub>, C<sub>6</sub>, C<sub>12</sub>).<sup>26</sup> Though, the reported  $T_g$  values were much higher and attributed to the 'hard' aromatic groups of DGEBA, ranging from 51 °C (C<sub>12</sub>) to 101 °C (C<sub>4</sub>) and from 89 °C (C<sub>12</sub>) to 96 °C (C<sub>2</sub>) for the diamines. However, all samples showed residual cure, which was also found by Xiao *et al.* in epoxidized sucrose esters-anhydride thermosets.<sup>27</sup> After 1 h of curing, all samples achieved 87-95% curing.

#### Polymer leaching study

**Scheme 1** Summary of possible interactions between ELO, DCAs and DMAP.

The weight percentage of the extracted soluble parts and their weight average molecular weight ( $M_w$ ) from films subjected to dissolution in CH<sub>2</sub>Cl<sub>2</sub> for 7 days are shown in Table 1. All the samples showed good solvent stability and the gel content was less than 2% for all the samples except C<sub>36</sub> sample which was 3%. The molecular weight of the soluble substances was about



2500 which indicated that the leachates were small molecules of the ring-opening products of ELO.

### FT-IR analysis

The reactions between epoxy and carboxyl groups are quite complex and esterification, etherification, condensation esterification and hydrolysis are all possible reactions.<sup>28</sup> Based on previous studies,<sup>29-32</sup> the possible interactions between ELO, DCAs and DMAP are proposed as shown in Scheme 1.

The infrared spectra of ELO, extracted soluble (leachate) and insoluble part (residue) of C<sub>6</sub> film are shown in Fig. 4. ELO clearly showed characteristic bands of the epoxy groups, oxirane C-O twin bands at 823 cm<sup>-1</sup> and 842 cm<sup>-1</sup>.<sup>33, 34</sup> The

ester stretching band was observed at 1742 cm<sup>-1</sup>. The other bands observed were: 723 cm<sup>-1</sup> (methylene in-phase rocking), 959 cm<sup>-1</sup>, 1010 cm<sup>-1</sup>, 1102 cm<sup>-1</sup> (ether, antisymmetric stretch), 1155 cm<sup>-1</sup>, 1240 cm<sup>-1</sup> (ester, antisymmetric stretch), 1379 cm<sup>-1</sup> (methyl symmetric deformation), 1463 cm<sup>-1</sup> (methyl antisymmetric deformation) and 2854 cm<sup>-1</sup>, 2923 cm<sup>-1</sup> (methylene symmetric and antisymmetric stretch).<sup>33</sup>

Compared with ELO, the characteristic oxirane absorption bands at 823 cm<sup>-1</sup> and 842 cm<sup>-1</sup> were not present in both cured products soluble and insoluble fractions. The carbonyl stretch band shifted from 1742 cm<sup>-1</sup> in ELO to 1738 cm<sup>-1</sup> for the extracted soluble sample and further shifted to 1732 cm<sup>-1</sup> in the

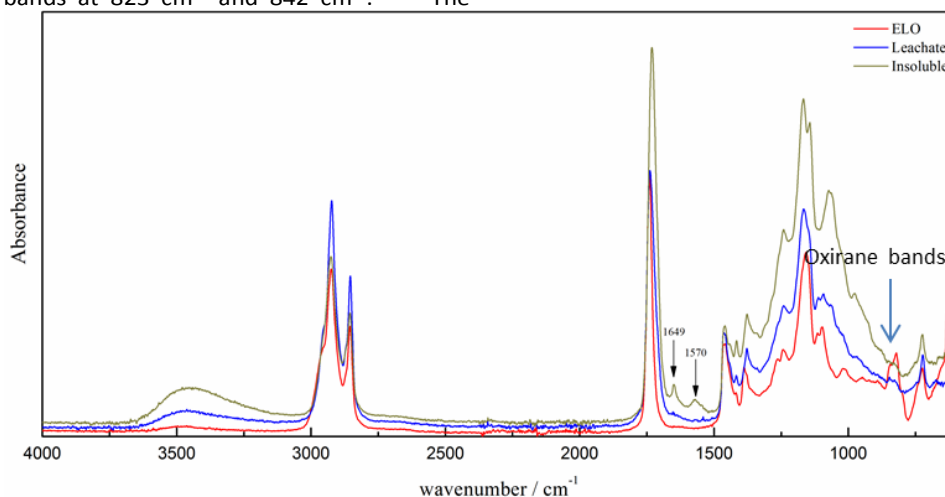


Fig. 4 FT-IR spectra of ELO, leachate and insoluble residue after extraction from cured C<sub>6</sub> film.

insoluble substances. Instead of a single band at 1155 cm<sup>-1</sup> in ELO, the ester C-O antisymmetric stretch band split into two bands (1168 cm<sup>-1</sup>, 1145 cm<sup>-1</sup>) in the insoluble samples and a band (1168 cm<sup>-1</sup>) and a shoulder (1145 cm<sup>-1</sup>) for the soluble samples. In addition, new ether group signals were found at 1073 and 979 cm<sup>-1</sup> in both the soluble and insoluble samples. These findings indicated that new ester and ether groups were formed between the acid group of DCAs and the epoxy groups of ELO. The DCM soluble substances are most likely low molecular weight ring-opening products of ELO, which have also been reported by Liu *et al.*<sup>35</sup>

The two bands at 1649 and 1570 cm<sup>-1</sup> in the insoluble product that remained after extraction have been attributed to the signals of protonated DMAP which, is linked to the carboxylate anion of these DCAs.<sup>19</sup> Interestingly, these two bands were not observed in the leachate, indicating that DMAP was not homogeneously dispersed in the resin system and therefore within these regions curing was not as effective and only smaller molecular DCM soluble clusters were formed.

### NMR analysis

The <sup>1</sup>H and <sup>13</sup>C NMR spectra of ELO and the cured extracted soluble fraction are shown in Fig. S1 and Fig. S2, respectively. <sup>1</sup>H NMR measurement on ELO indicated that the epoxy group was present from the signal in the δ 3.0-3.2 ppm region. The ELO base sample also showed signals at δ 5.1-5.3 ppm and 4.0-

4.4 ppm which correlate to the methine proton of -CH<sub>2</sub>-CH-CH<sub>2</sub>- and methylene proton of -CH<sub>2</sub>-CH-CH<sub>2</sub>- of glycerol's backbone, respectively. Other signals include CH<sub>2</sub> proton adjacent to two epoxy group at δ 2.8-3.0 ppm, α-CH<sub>2</sub> to carbonyl group at δ 2.2-2.4 ppm, α-CH<sub>2</sub> to epoxy ring at δ 1.7-1.9 ppm, β-CH<sub>2</sub> to carbonyl group at δ 1.55-1.7 ppm, β-CH<sub>2</sub> to epoxy ring at δ 1.4-1.55 ppm, saturated methylene group at δ 1.1-1.4 ppm and terminal -CH<sub>3</sub> groups at δ 0.8-1.0 ppm.<sup>36</sup> Compared with ELO, the characteristic epoxy signals at δ 3.0-3.2 were absent in the leachate sample suggesting no unreacted ELO was present post curing and verifying the findings from the FT-IR analysis. The peak at δ 2.8-3.0 ppm changed from a multiple peak to a single peak which further confirmed the ring-opening reaction. The disappearance of peak at δ 0.9-1.0 ppm was attributed to the CH<sub>3</sub> of the linoleic acid.<sup>37</sup>

<sup>13</sup>C NMR measurement on ELO indicated that the epoxy group is present in the δ 54-58 ppm region. The presence of <sup>13</sup>C NMR peak at 173.1 ppm was due to carbonyl carbon of triacylglycerol and peaks at 68.9 ppm and 62.1 ppm, respectively, assigned to methine carbon of -CH<sub>2</sub>-CH-CH<sub>2</sub>- and methylene carbon of -CH<sub>2</sub>-CH-CH<sub>2</sub>- backbone. Again, compared with ELO the extracted soluble substances did not show the characteristic epoxy peaks in the δ 54-58 ppm region. Solid state <sup>13</sup>C-NMR of the insoluble substances clearly showed the existence of carbonyl/ester groups at 174 ppm, which was also

complemented by presence of C=O str of an ester as shown in the FTIR spectrum (Fig. 4)

### Mechanical properties

Fig. 5 shows the relationship between stress and strain of the cured ELO-DCA products. Except for the sample cured with adipic acid ( $C_6$ ), all others show a linear relationship between stress and strain. In this case, strain hardening can be observed helping to account for its much higher mechanical properties.

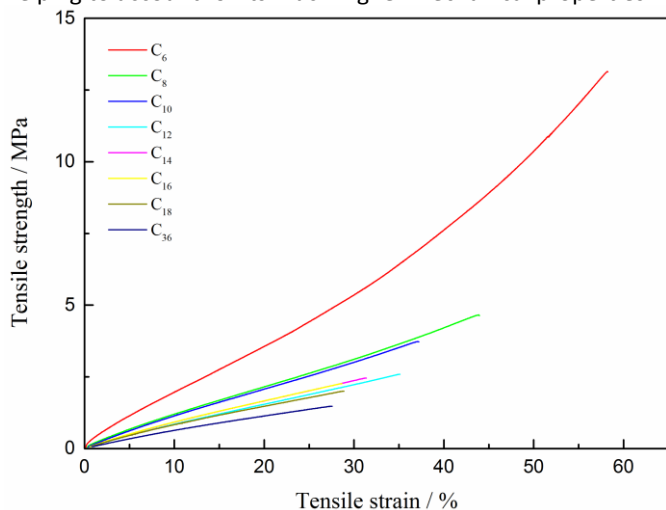


Fig. 5 Strain-stress curves of cured films with different DCAs.

The reason for strain hardening is possibly related to the orientation effects during tensile strain. The longer DCAs chains could prevent this orientation effect and hence, explaining their marked decrease in mechanical properties. Strain hardening has also been observed in adipate polyurethane elastomers which was explained by the crystallization/orientation of the amorphous polyol chains during the applied strain.<sup>38</sup>

Fig. 6 shows the effect of different DCAs on the mechanical properties of the obtained thermosetting resins. The film derived from adipic acid ( $C_6$ ) has the best mechanical properties with elongation at break of 55%, tensile strength of 8.8 MPa, Young's modulus of 22.0 MPa and toughness of 3.1 MJ m<sup>-3</sup>. The mechanical properties after  $C_6$  as mentioned previously

can be seen to dramatically decrease initially, and then gradually decrease with increasing chain length. The elongation properties of the materials however, after a DCA chain length of  $C_{10}$ , remained constant around 30%. Compared with the  $C_6$  film that derived from Pripol 1009F ( $C_{36}$ ) had the poorest tensile strength (1.1 MPa), Young's modulus (4.70 MPa) and toughness (0.2 MJ m<sup>-3</sup>) due to longer chain of Pripol increasing the free volume of the polymer, plasticising the network.

Additional differences in the mechanical properties of these materials with DCA chain length could be related to the films cured with shorter DCAs having a  $T_g$  close to RT and still within the leathery material zone ( $T_g$  10 ± °C), and as such, will show better mechanical properties than those in the rubbery state.<sup>39</sup> Though, tensile strength and elongation of DGEBA cured with various DCAs in the absence of accelerators were reported by Shimbo *et al.*,<sup>17</sup> which showed that tensile strength and elongation decreased with increase of chain length except for  $C_6$  adipic acid that gave the worst elongation. Shimbo *et al.* also showed that the tensile strength and elongation were 62 MPa and 5.1%, respectively. The much higher tensile strength and lower elongation properties were attributed to the aromatic structure and the higher crosslink density caused by the end epoxy groups with in DGEBA molecules. Yang *et al.*<sup>40</sup> reported that epoxy resins cured with shorter diamines (Jeffamine D-230) had better tensile strength and modulus but poorer elongation at break compared with longer diamines (Jeffamine D-400).

### DMA analysis

DMA tests were undertaken at five different frequencies 1, 3, 7, 10 and 20 Hz. Table 2 and Table S2 compares the dependencies of storage modulus and loss modulus on temperature for the epoxy cured with different DCAs, and the  $T_g$  was defined as the peak temperature of loss modulus. Due to the large change in the storage modulus after the  $T_g$  and the sample thickness limitations the values generated after this point were deemed invalid and beyond the test limit of the instrument. However, similar to the tests carried out at RT on the Instron the storage modulus below the  $T_g$  decreased with increasing DCA chain

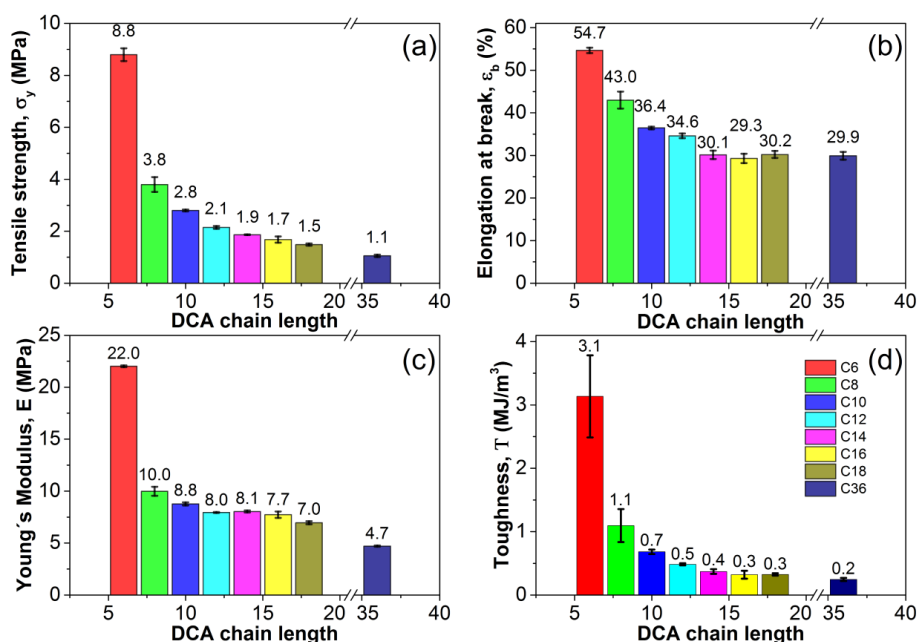


Fig. 6 Mechanical properties of films with different DCAs, (a) tensile strength; (b) elongation at break; (c) Young's modulus; and (d) toughness.

Table 2. Storage modulus and  $T_g$  of samples tested at 1 Hz and calculated activation energy  $E_\beta$ .

| Sample          | Storage modulus [MPa] |        |        |        |        |      | $T_g$ [°C] | $E_\beta$ [kJ·mol <sup>-1</sup> ] |
|-----------------|-----------------------|--------|--------|--------|--------|------|------------|-----------------------------------|
|                 | -100 °C               | -80 °C | -60 °C | -40 °C | -20 °C | 0 °C |            |                                   |
| C <sub>6</sub>  | 4348                  | 3673   | 3219   | 2889   | 2482   | 1228 | 1.5        | 67.1                              |
| C <sub>8</sub>  | 3231                  | 2732   | 2416   | 2182   | 1872   | 568  | -2.9       | 54.5                              |
| C <sub>10</sub> | 2387                  | 1976   | 1735   | 1582   | 1390   | 302  | -3.8       | 53.5                              |
| C <sub>12</sub> | 1634                  | 1339   | 1180   | 1090   | 969    | 115  | -7.5       | 49.4                              |
| C <sub>14</sub> | 2386                  | 2060   | 1869   | 1726   | 1497   | 62   | -8.2       | 43.7                              |
| C <sub>16</sub> | 2856                  | 2395   | 2128   | 1986   | 1686   | 173  | -9.0       | 48.0                              |
| C <sub>18</sub> | 2179                  | 1902   | 1750   | 1675   | 1468   | 30   | -10.9      | 57.3                              |
| C <sub>36</sub> | 2195                  | 1929   | 1722   | 1492   | 664    | 5    | -19.0      | 59.9                              |

length due to decreased crosslink density, with the C<sub>6</sub> sample showing the highest storage modulus over the analysed range of -100 to 0 °C.

However, similar to the mechanical testing (Fig. 6) there was a considerable decrease (33% ± 1, not including 0 °C to limit transition effects) in the storage modulus changing from the C<sub>6</sub> sample to the C<sub>8</sub>, though not as significant as the decline (132%) observed in tensile strength. This further supports that the C<sub>6</sub> sample was analysed while partially in the leathery region and/ or additional orientation effects occurred during the RT (Instron) testing.

$T_g$  of these samples tested by DMA were in the same trend with DSC results and the shorter chain sample had the higher

$T_g$ . The activation energy of the beta transition,  $E_\beta$ , was obtained by applying the Arrhenius law (equation 2).<sup>41</sup>

$$E_\beta = -R \left[ \frac{d(\ln f)}{d(1/T_\beta)} \right] \quad (2)$$

by plotting of  $\ln f$  versus  $1/T_\beta$  as shown in Fig. S3 whereby the gradient corresponds to  $E_\beta$ .

Table 2 shows that the activation energy for the  $\beta$  transition, i.e., approximately 55 kJ mol<sup>-1</sup> is similar to that reported by Boquilon *et al.*,<sup>42</sup> of 63 kJ mol<sup>-1</sup> for a ELO-THPA (*cis*-1,2,3,6-tetrahydrophthalic anhydride) system. The presence of a  $\beta$  transition can be seen for all samples with those prepared with a shorter DCAs having a higher intensity than those prepared from the longer DCAs as can be seen in the ESI, Fig. S4. For

some materials it has been shown that there is an interrelationship with its proportion and to the general mechanical properties (toughness) of the materials tested. In this case, there is a broad correlation with the shorter chain length DCAs having a higher  $\tan \delta$  intensity, and the longer DCAs a weaker intensity and poorer storage modulus. For these types of materials the  $\beta$  the motion of the diester segments formed between two crosslinks.<sup>43</sup>

### Thermal stability

The thermal stability profiles as determined by thermogravimetric analysis (TGA) of the obtained epoxy resins are shown in Fig. 7 and summarised in Table 3.

All films showed similar degradation behaviour in both  $N_2$  and air with good thermal stability, i.e.,  $T_5$  (5% weight loss temperature) ranging from 347 °C to 369 °C in  $N_2$  and 337 °C to 348 °C in air. A weight loss of 94%-99% was obtained at temperatures up to 600 °C. From Table 3, it's shown that the decomposition temperatures and residue at 450 °C increased with the increase of chain length. Resins cured with longer chain length of DCAs had better thermal stability due to the more bonds to absorb and dissipate energy for internal re-ordering. Vilela *et al.*<sup>44</sup> studied the thermal stability of polyesters prepared from  $C_{26}$  dicarboxylic acid with different chain length of diols ( $C_4$ ,  $C_{12}$ ,  $C_{26}$ ) and their study confirmed that better thermal stability was obtained with higher chain length of polyesters.

Table 3 Thermal stability of the cured epoxy resins in  $N_2$  and air (Italics).

| Sample          | $T_5$<br>[°C] | $T_{10}$<br>[°C] | $T_{50}$<br>[°C] | $T_{max}$<br>[°C] | $R_{300}$<br>[%] | $R_{450}$<br>[%] | $R_{600}$<br>[%] |
|-----------------|---------------|------------------|------------------|-------------------|------------------|------------------|------------------|
| C <sub>6</sub>  | 347.4         | 363.7            | 403.2            | 391.8             | 98.5             | 17.8             | 6.0              |
|                 | <i>337.5</i>  | <i>360.1</i>     | <i>406.3</i>     | <i>400.4</i>      | <i>98.1</i>      | <i>19.8</i>      | <i>1.0</i>       |
| C <sub>8</sub>  | 357.1         | 368.6            | 403.0            | 391.3             | 99.6             | 17.6             | 3.6              |
|                 | <i>334.9</i>  | <i>359.0</i>     | <i>406.2</i>     | <i>401.1</i>      | <i>97.6</i>      | <i>21.7</i>      | <i>2.4</i>       |
| C <sub>10</sub> | 356.1         | 368.5            | 405.6            | 391.7             | 99.0             | 20.4             | 5.1              |
|                 | <i>332.2</i>  | <i>360.1</i>     | <i>404.3</i>     | <i>401.4</i>      | <i>97.1</i>      | <i>19.6</i>      | <i>1.0</i>       |
| C <sub>12</sub> | 359.6         | 371.4            | 406.3            | 390.5             | 99.5             | 19.2             | 1.3              |
|                 | <i>337.0</i>  | <i>363.8</i>     | <i>405.0</i>     | <i>404.6</i>      | <i>97.6</i>      | <i>18.9</i>      | <i>1.9</i>       |
| C <sub>14</sub> | 357.1         | 370.6            | 408.8            | 401.8             | 99.0             | 24.7             | 5.1              |
|                 | <i>337.2</i>  | <i>363.8</i>     | <i>406.1</i>     | <i>404.9</i>      | <i>98.0</i>      | <i>20.0</i>      | <i>1.1</i>       |
| C <sub>16</sub> | 357.4         | 371.3            | 410.3            | 395.1             | 99.0             | 25.6             | 6.8              |
|                 | <i>337.4</i>  | <i>366.7</i>     | <i>414.6</i>     | <i>404.3</i>      | <i>97.8</i>      | <i>26.6</i>      | <i>2.4</i>       |
| C <sub>18</sub> | 362.7         | 374.9            | 412.5            | 397.4             | 99.6             | 27.1             | 5.3              |
|                 | <i>337.9</i>  | <i>365.0</i>     | <i>417.3</i>     | <i>400.5</i>      | <i>97.7</i>      | <i>29.4</i>      | <i>3.9</i>       |
| C <sub>36</sub> | 368.8         | 380.0            | 423.5            | 402.7             | 99.5             | 31.4             | 3.3              |
|                 | <i>348.4</i>  | <i>378.3</i>     | <i>412.1</i>     | <i>404.2</i>      | <i>98.9</i>      | <i>28.6</i>      | <i>2.3</i>       |

Fig. 7 (a) clearly shows that the resins experienced a two-stage decomposition process in  $N_2$ . Since these two stages show the same decomposition profile in both  $N_2$  and air, they were caused by the scission of ester linkages.<sup>45</sup> The first stage from 350 °C to 430 °C resulted from chain scission in the linseed oil ester groups which was confirmed by the decomposition process of pure ELO.<sup>29, 46</sup> While the second stage beyond 430 °C resulted from the ester groups formed by the ring-opening reactions between DCAs and epoxy groups. With the increase of chain length, the second stage became more apparent. Under oxidative conditions, the decomposition process is more complex with an additional higher temperature main stage of the decomposition occurring beyond 500 °C, which corresponds to the further oxidation of the residual char.<sup>47</sup>

### Conclusions



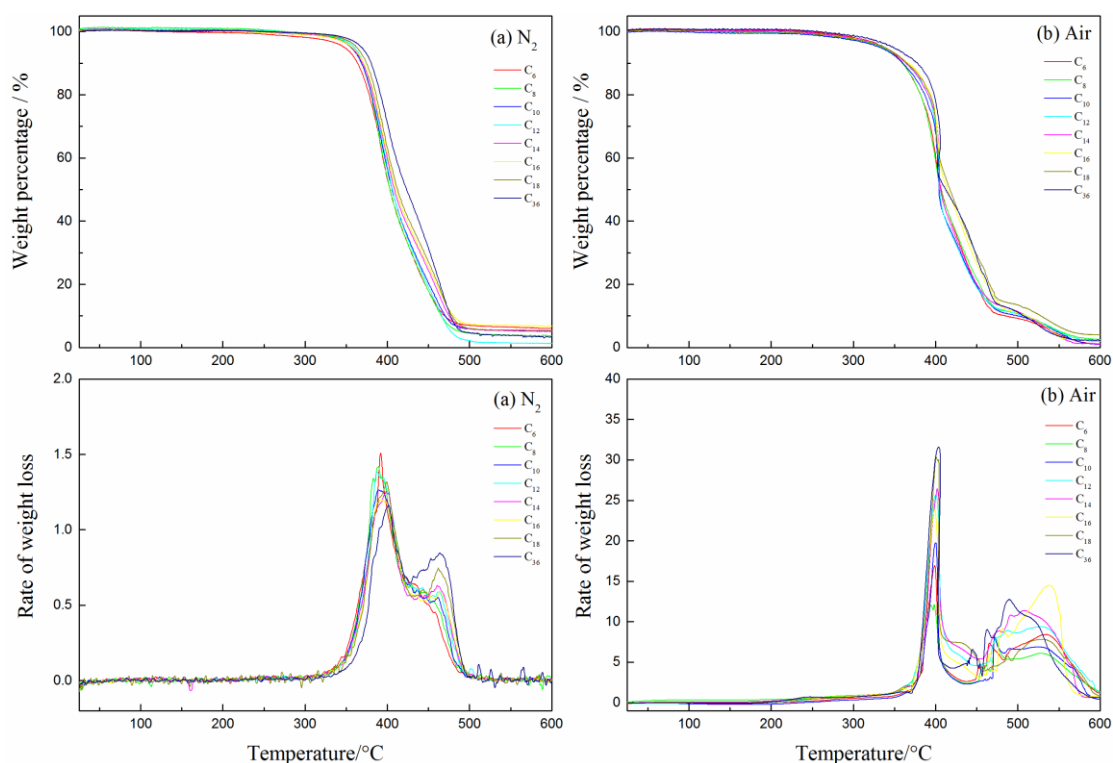


Fig. 7 TGA and DTG of ELO-DCA films in (a)  $N_2$  and (b) air at  $10\text{ }^\circ\text{C min}^{-1}$  heating rate.

In conclusion biobased thermoset resins were obtained from ELO and bio-derived dicarboxylic acids. The effects of chain length on the properties of thermoset resins were studied by various methods, DSC, FT-IR, NMR, DMA, mechanical test and TGA. All resins were flexible and transparent with good thermal stability and solvent stability. The results showed that shorter chain diacid had better reactivity towards epoxide groups. Resins with shorter chain length DCAs showed higher  $T_g$  and better mechanical properties including tensile strength, tensile strain, modulus and toughness but poorer thermal stability. More interestingly, strain hardening was observed in samples prepared with adipic acid that helped account for the much higher RT mechanical properties compared to other samples.

## Experimental

### Materials

ELO (Lankroflex® L, oxirane content = 9.0%) was obtained from Akcros Chemicals, Eccles, England. The  $C_6$ - $C_{16}$  diacids were purchased from Sigma Aldrich:  $C_6$  adipic acid (99.5%),  $C_8$  suberic acid (98%),  $C_{10}$  sebacic acid (99%),  $C_{12}$  dodecanedioic acid (99%),  $C_{14}$  tetradecanedioic acid (98%),  $C_{16}$  hexadecanedioic acid (96%). Octadecanedioic acid (95%) was purchased from Fluorochem and bio-derived  $C_{36}$  diacid (Pripol 1009F, acid value 194 mg KOH/g) was kindly supplied by Croda. Oxalic acid ( $C_2$ ) and succinic acid ( $C_4$ ) were not used due to their high melting point, i.e.,  $189.5\text{ }^\circ\text{C}$  and  $185\text{ }^\circ\text{C}$ , respectively. 4-*N,N*-Dimethylaminopyridine (DMAP) was purchased from Sigma Aldrich. All chemicals were used as received without further purification.

### Film preparation

All samples were prepared with a stoichiometric relationship,  $R$ , of 0.7 ( $R = \text{acid groups/epoxy groups}$ ).<sup>19</sup> For each formulation, the amount of DMAP added was calculated based on 1 mol% of epoxy functional groups. The mixture was stirred at  $150\text{ }^\circ\text{C}$  for 5 min, poured into a hot aluminum pan (internal diameter, 70 mm) and cured in a fan-assisted oven at  $160\text{ }^\circ\text{C}$  for 1 h.

### DSC analysis

The DSC analyses were performed with a TA Instruments Q2000 DSC. Premixed samples (7-10 mg), obtained after stirring at  $150\text{ }^\circ\text{C}$  for 5 min, were hermetically-sealed in Tzero aluminum DSC pans. Thermal runs were performed under a constant flow of dry nitrogen ( $50\text{ mL min}^{-1}$ ). Dynamic runs were performed under four different heating rates, 5, 10, 15 and  $20\text{ }^\circ\text{C min}^{-1}$ , over a temperature range of  $25\text{ }^\circ\text{C}$  to  $320\text{ }^\circ\text{C}$ . The results reported are the averages of the three measurements. Glass transition temperature  $T_g$  was obtained by heat-cool cycling ( $10\text{ }^\circ\text{C min}^{-1}$ ) of the cured resins (7-10 mg) sealed in Tzero aluminum hermetic DSC pans.

### Polymer leaching study

Approximately 2 g cured sample was subjected to leaching in dichloromethane (DCM, 20 mL) at room temperature for 7 days. Thereafter, the leachate was concentrated *in vacuo* and both leachate and residue were dried overnight at room temperature under vacuum. The leachate was analysed by GPC, FT-IR and NMR whereas residues were characterized by FT-IR and solid state  $^{13}\text{C}$  NMR only. The sol content (%) was

determined as the average of two measurements using the equation below

$$\% \text{ sol content} = 100 \times \left( \frac{w_t - w_{\text{gel}}}{w_t} \right) = 100 \times \frac{w_{\text{sol}}}{w_t}$$

where  $w_t$  is the total weight of thermoset sample,  $w_{\text{gel}}$  is the weight of residue after extraction (gel fraction) and  $w_{\text{sol}}$  is the weight of loss during extraction (sol fraction).

#### ATR-IR analysis

ATR-IR (attenuated total reflection infrared) spectra were recorded on a Bruker Vertex 70 Spectrometer equipped with a diamond golden gate ATR cell over a scanning range of 600–4000  $\text{cm}^{-1}$  for 32 scans at a spectral resolution of 2  $\text{cm}^{-1}$ .

#### NMR analysis

$^1\text{H}$  and  $^{13}\text{C}$  NMR spectra for starting materials and extracted soluble materials were recorded on a JEOL JNM-ECS 400 MHz spectrometer. Solid state  $^{13}\text{C}$  NMR (CPMAS) spectra for insoluble parts were acquired using a 400 MHz Bruker Avance III HD spectrometer equipped with a Bruker 4mm H(F)/X/Y triple resonance probe and 9.4T Ascend<sup>®</sup> superconducting magnet. The experiment employed a 1.0 ms linearly-ramped contact pulse, spinning rate of 10000  $\pm$  2 Hz, optimized recycle delay of 7 seconds, spinal-64 heteronuclear decoupling (at  $\nu_{\text{rf}}=85$  kHz) and is a sum of 600 co-added transients. Chemical shifts are reported with respect to tetramethylsilane (TMS) and were referenced using adamantane (29.5 ppm) as an external secondary reference.

#### GPC analysis

GPC was performed at 40 °C in tetrahydrofuran (THF) stabilised with 0.025% tert-butylated hydroxytoluene (BHT) with eluent pumped at the constant flow rate of 1.0  $\text{mL min}^{-1}$ . The samples were analysed using a PL-GPC 50 system equipped with PLGel column guard and 3x PLGel 5 $\mu\text{m}$  mixed bed-C columns (300 x 7.5 mm). Before injecting the samples, the system was calibrated by performing Universal Calibration with single PL-polystyrene standard and a set of PL-EasyVial PS-H polystyrene standards of molecular known molecular weights. Viscometry (PL-BV 400RT viscometer) and refractometry (PL-RI differential refractometer) were used as detectors and the resultant data was processed by Varian 'Cirrus Multi detector' software.

#### DMA analysis

Thermal relaxations of the cross-linked bioplastics were carried out on a dynamic mechanical analyser (DMA Q800, TA Instruments) using a 3-point bending mode accessory at 1, 3, 7, 10 and 20 Hz. Samples with dimensions of 20x10 mm with a film thickness ranging from 1 – 1.5 mm (thinner than recommended due to sample preparation constraints) were heated from -120 to 50 °C at a heating rate of 1 °C  $\text{min}^{-1}$ .

#### Mechanical properties

Standard dumb-bell shapes (60 mm x 10 mm) were cut with film thickness in the region of 1–1.5 mm. Tensile tests were

conducted using an Instron 3367 universal testing machine fitted with 1000 N capacity load cell. The initial grip separation was set at 35 mm and the crosshead speed was 20  $\text{mm min}^{-1}$ . The results reported were the average of the three measurements.

#### Thermal stability

The thermal stability of the cured resins was analyzed using simultaneous thermal analyser (Stanton Redcroft STA 625). Approximately 10 mg of the sample was heated from room temperature to 600 °C at a heating rate of 10 °C  $\text{min}^{-1}$  under nitrogen and air atmospheres, respectively.

#### Acknowledgements

C. Ding would like to acknowledge the Department of Chemistry, University of York, for a Wild Fund scholarship for PhD study. We would like to acknowledge Akros Chemical for the generous supply of ELO and Croda for the supply of Pripol 1009F. We would like to acknowledge Dr. Pedro M. Aguiar at the Department of Chemistry, University of York, for his kind help with solid state CP-MAS  $^{13}\text{C}$  NMR analysis. In addition, financial support from the Ministerio de Ciencia e Innovación (MICINN, Project MAT2010-21070-C02-01) is gratefully acknowledged. P. Shuttleworth would like to thank to the MICINN for a Juan de la Cierva postdoctoral contract (JCI-2011-10836).

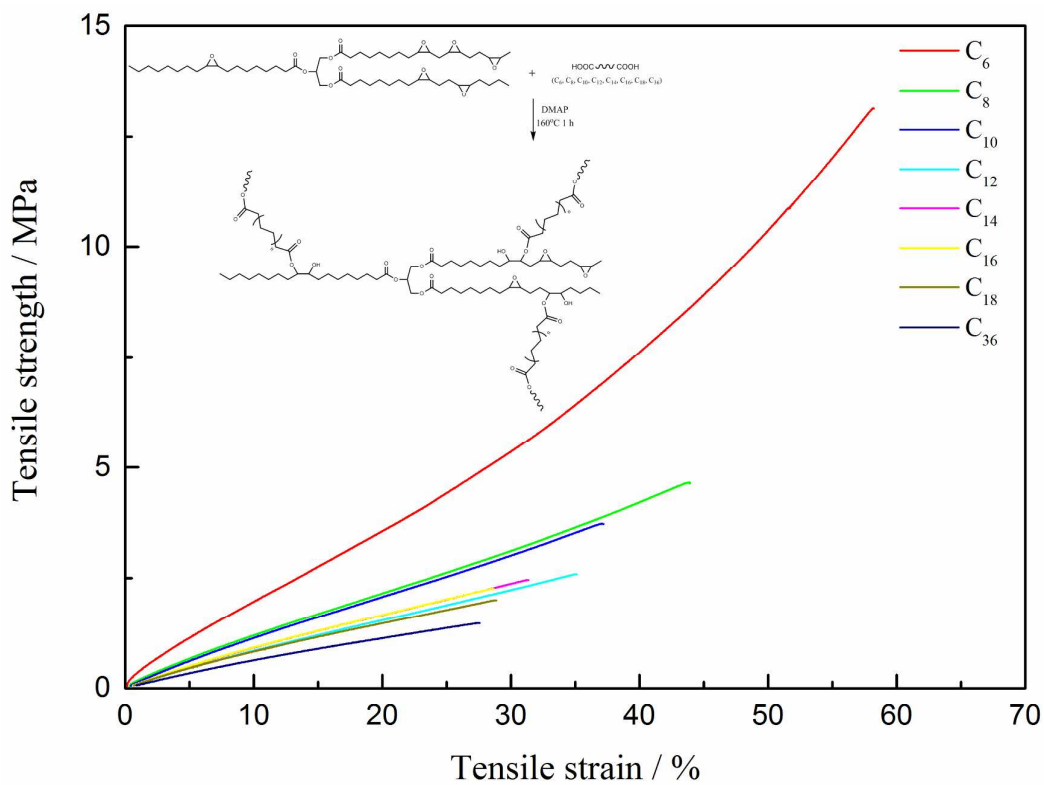
#### References

1. J. Bozell Joseph, in *Chemicals and Materials from Renewable Resources*, American Chemical Society, 2001, vol. 784, ch. 1, pp. 1-9.
2. J. Bozell Joseph, in *Feedstocks for the Future*, American Chemical Society, 2006, vol. 921, ch. 1, pp. 1-12.
3. A. Gandini and M. N. Belgacem, in *Monomers, Polymers and Composites from Renewable Resources*, eds. M. N. Belgacem and A. Gandini, Elsevier, Amsterdam, 2008, pp. 1-16.
4. *Bioplastics: technologies and global markets*, BBC research reports PLS050C, 2014. <http://www.bccresearch.com/market-research/plastics/bioplastics-pls050c.html>. Accessed 260415.
5. *Final evaluation of the lead market initiative*, Centre for strategy & evaluation services, 2011.
6. <http://www.biopREFERRED.gov/BioPreferred/faces/pages/AboutBioPreferred.xhtml>, Accessed 260115.
7. L. Shen, J. Haufe and M. K. Patel, *Product overview and market projection of emerging bio-based plastics PRO-BIP 2009*, Utrecht University, 2009.
8. PERP program - epoxy resins. Nexant Chem Systems, 2006. [http://www.chemsystems.com/reports/search/docs/abstracts/0405S11\\_abs.pdf](http://www.chemsystems.com/reports/search/docs/abstracts/0405S11_abs.pdf), Accessed 270214, 2014.
9. R. Auvergne, S. Caillol, G. David, B. Boutevin and J.-P. Pascault, *Chem. Rev.*, 2013, **114**, 1082-1115.
10. C. Ding and A. S. Matharu, *ACS Sustainable Chemistry & Engineering*, 2014, **2**, 2217-2236.

11. Top value added chemicals from biomass volume I - results of screening for potential candidates from sugars and synthesis gas. U.S. Department of Energy, vol. 2013.
12. Y. Xu, M. A. Hanna and L. Isom, *The Open Agricultural Journal*, 2008, **2**, 54-61.
13. A. Corma, S. Iborra and A. Velty, *Chem. Rev.*, 2007, **107**, 2411-2502.
14. E. d. Jong, A. Higson, P. Walsh and M. Wellisch, *Bio-based chemicals: value added products from biorefineries*, IEA Bioenergy, 2012.
15. F. W. Lichtenthaler, in *Ullmann's Encyclopedia of Industrial Chemistry*, Wiley-VCH Verlag GmbH & Co. KGaA, 2000.
16. J. O. Metzger, *Eur. J. Lipid Sci. Technol.*, 2009, **111**, 865-876.
17. M. Shimbo, M. Ochi and Y. Konishi, *Zairyo*, 1979, **28**, 319-325.
18. R. Shogren, Z. Petrovic, Z. Liu and S. Erhan, *J. Polym. Environ.*, 2004, **12**, 173-178.
19. N. Supanchaiyamat, P. S. Shuttleworth, A. J. Hunt, J. H. Clark and A. S. Matharu, *Green. Chem.*, 2012, **14**, 1759-1765.
20. D. Montarnal, M. Capelot, F. Tournilhac and L. Leibler, *Science*, 2011, **334**, 965-968.
21. M. Capelot, D. Montarnal, F. Tournilhac and L. Leibler, *J. Am. Chem. Soc.*, 2012, **134**, 7664-7667.
22. M. Capelot, M. M. Unterlass, F. Tournilhac and L. Leibler, *ACS Macro Letters*, 2012, **1**, 789-792.
23. P. G. Laye, in *Principles of Thermal Analysis and Calorimetry*, The Royal Society of Chemistry, 2002, pp. 55-93.
24. Y.-C. Chiu, C.-C. Huang, H.-C. Tsai, A. Prasanna and I. Toyoko, *Polym. Bull.*, 2013, **70**, 1367-1382.
25. G. Mashouf Roudsari, A. K. Mohanty and M. Misra, *ACS Sustainable Chemistry & Engineering*, 2014, **2**, 2111-2116.
26. M. Shimbo, M. Ochi and Y. Shigeta, *J. Appl. Polym. Sci.*, 1981, **26**, 2265-2277.
27. X. Pan, P. Sengupta and D. C. Webster, *Biomacromolecules*, 2011, **12**, 2416-2428.
28. L. Shechter and J. Wynstra, *Industrial & Engineering Chemistry*, 1956, **48**, 86-93.
29. N. Supanchaiyamat, A. J. Hunt, P. S. Shuttleworth, C. Ding, J. H. Clark and A. S. Matharu, *RSC Advances*, 2014, **4**, 23304-23313.
30. P.-J. Madec and E. Maréchal, in *Analysis/Reactions/Morphology*, Springer Berlin Heidelberg, 1985, vol. 71, ch. 4, pp. 153-228.
31. C. E. Hoppe, M. J. Galante, P. A. Oyanguren and R. J. J. Williams, *Macromolecular Materials and Engineering*, 2005, **290**, 456-462.
32. I. E. Dell'Erba and R. J. J. Williams, *Polymer Engineering & Science*, 2006, **46**, 351-359.
33. A. Adhvaryu and S. Z. Erhan, *Ind. Crop. Prod.*, 2002, **15**, 247-254.
34. A. R. Mahendran, N. Aust, G. Wuzella and A. Kandelbauer, *Macromol. Symp.*, 2012, **311**, 18-27.
35. Z. Liu and S. Erhan, *Journal of the American Oil Chemists' Society*, 2010, **87**, 437-444.
36. P. S. Lathi and B. Mattiasson, *Applied Catalysis B: Environmental*, 2007, **69**, 207-212.
37. O. Zovi, L. Lecamp, C. Loutelier-Bourhis, C. M. Lange and C. Bunel, *Green. Chem.*, 2011, **13**, 1014-1022.
38. E. Honcoop and E. Appelman, *European Coatings Journal*, 2002, **9**, 1-6.
39. J. Hong, Q. Luo, X. Wan, Z. S. Petrović and B. K. Shah, *Biomacromolecules*, 2011, **13**, 261-266.
40. G. Yang, S.-Y. Fu and J.-P. Yang, *Polymer*, 2007, **48**, 302-310.
41. L. Barral, J. Cano, A. López, P. Nogueira and C. Ramírez, *J. Therm. Anal.*, 1994, **41**, 1463-1467.
42. N. Boquillon and C. Fringant, *Polymer*, 2000, **41**, 8603-8613.
43. Z. S. Petrović, W. Zhang and I. Javni, *Biomacromolecules*, 2005, **6**, 713-719.
44. C. Vilela, A. J. D. Silvestre and M. A. R. Meier, *Macromol. Chem. Phys.*, 2012, **213**, 2220-2227.
45. J.-M. Pin, N. Sbirrazzuoli and A. Mija, *ChemSusChem*, 2015, **8**, 1232-1243.
46. C. Zhang, Y. Li, R. Chen and M. R. Kessler, *ACS Sustainable Chemistry & Engineering*, 2014, **2**, 2465-2476.
47. B. Yu, Y. Shi, B. Yuan, S. Qiu, W. Xing, W. Hu, L. Song, S. Lo and Y. Hu, *Journal of Materials Chemistry A*, 2015, **3**, 8034-8044.

## New insights into the curing of epoxidized linseed oil with dicarboxylic acids

Cheng Ding,<sup>a</sup> Peter S. Shuttleworth,<sup>b</sup> Sarah Makin,<sup>a</sup> James H. Clark<sup>a</sup> and Avtar S. Matharu<sup>a</sup>



A systematic study of the synthesis and characterization of epoxy thermosets derived from ELO cured with different DCAs in the presence of DMAP at 160 °C for 1 h.